Attosecond Technology and Science

Giuseppe Sansone, Francesca Calegari, and Mauro Nisoli

(Invited Paper)

***Abstract*—The generation of attosecond pulses has been the result of tremendous efforts and advances in the field of the interaction of ultrashort intense laser pulses with matter. Nowadays, the electric field waveform of femtosecond pulses can be precisely controlled and used to synthesize and measure the evolution in time of attosecond pulses. The quest for increasing photon fluxes in the extreme-ultraviolet region (XUV) and the requirement of a complete characterization of complex attosecond waveforms are stimulating the development of new technological approaches that should make feasible XUV sources combining attosecond pulse duration, high energy, and high repetition rate. The use of such sources with state-of-the-art techniques for the measurement of the momentum of charged particles will allow a detailed description of photoionization and photodissociation processes. Advances in selection of the initial quantum state and structure of molecules will open the way for the extension of attosecond spectroscopy to complex molecules. The first applications of attosecond pulses allowed the investigation of electron dynamics with a resolution close to the atomic unit of time. Simple systems such as helium and noble gases were investigated using trains and isolated pulses. These experiments represent benchmarks to elucidate the response of atoms on the typical electron timescale.**

***Index Terms*—Lasers, laser and electrooptics, optics, ultrafast optics.**

I. Introduction

THE internal dynamics of the constituents of complex systems can be investigated by means of pump–probe techniques: in this general scheme, a pump (a collision with a neutral or charged particle, the absorption or scattering of a photon, etc.) initiates a dynamics that can be probed at a later (usually controllable) time by a probe event. The smallest features in time that can be observed, i.e., the time resolution that can be achieved, are determined by the durations of the pump and probe events. Nowadays, the shortest events that can be generated in a controllable way are represented by bursts of light in the extreme-ultraviolet region (XUV), which can extend down to 80 as (1 as $= 10^{-18}$ s) [1]. The generation and characterization of such pulses have been achieved through several efforts in the field of ultrafast intense laser sources over the past 20 years [2] and through theoretical developments on the interaction of intense light pulses with atomic and molecular systems [3]. The duration of attosecond pulses is rapidly approaching the atomic unit of time [4], [5] that represents, in the classical description of the atomic model, the natural time scale of the electronic motion; also in quantum mechanics the attosecond regime is the relevant time domain for electrons as the inverse of the energy spacing among electronic levels, (that determines the time constant for nonstationary states), lies typically in this range. Used as a pump, attosecond pulses, due to their large energy bandwidth, offer the possibility to excite coherently different electronic levels or bands inside atoms [6], molecules [7], and solids [8]; on the other hand, used as a probe, they allow to take snapshots of the time evolution of the electronic motion [9], [10]. The combination of attosecond pulses for both steps has been limited by the low energy content usually associated with isolated pulses (typically picojoule range) and has prevented, so far, the development of nonlinear attosecond spectroscopy. For other experiments, however, the main limitation is not represented by the achievable XUV intensity, but by the low cross section of the reaction channels under investigation that requires the application of complex spectroscopic techniques to measure the desired physical observables. Indeed, due to the broad bandwidth associated with attosecond pulses, a large variety of electronic levels can be simultaneously accessed and several reaction channels can be observed in the same experiment. In order to disentangle the contributions of the various mechanisms, a precise characterization of the particles involved in the reaction is required. This characterization can be achieved by using spectrometers for electrons and ions measuring the momentum distributions of a single or of all particles involved in the reaction. Because in many conditions the channel to be investigated is not the dominant one, accumulation of several events and appropriate sorting out of the data is necessary. This condition translates into data integration time that renders several experiments unfeasible because of stability issues of the experimental conditions (mainly related to the driving laser sources) over extended time periods. For such applications the main limitation turns out to be the repetition rate of the attosecond source that is typically limited to a few kHz because of the high intensity of the driving pulses required for the generation of harmonic radiation in gases.

In this study, the latest technological advances toward the demonstration of experimental apparatus suited for the investigation of attosecond dynamics based on measurement

Manuscript received November 4, 2010; revised February 17, 2011; accepted April 11, 2011. Date of publication September 8, 2011; date of current version January 31, 2012. This work was supported in part by the Italian Ministry of Research under project FIRB RBID08CRXK, in part by the European Union under Contract 228334 JRA-ALADIN (Laserlab Europe II) and Contract MC-RTN ATTOFEL (FP7-238362), in part by the European Research Council under the European Community's Seventh Framework Programme (FP7/2007-2013) under ERC grant 227355-ELYCHE, and in part by the Ateneo italo-tedesco (Programma-Vigoni 2007–2009). The work of G. Sansone was supported by the Alexander von Humboldt Foundation under project "Tirinto."

G. Sansone was with the Max Planck Institut für Kernphysik, 69117 Heidelberg, Germany. He is now with the CNR-IFN Dipartimento di Fisica Politecnico Milano, 20133 Milano, Italy (e-mail: giuseppe.sansone@polimi.it).

F. Calegari and M. Nisoli are with the CNR-IFN Dipartimento di Fisica Politecnico Milano, 20133 Milano, Italy.

Color versions of one or more of the figures in this paper are available online at http://ieeexplore.ieee.org.

Digital Object Identifier 10.1109/JSTQE.2011.2153181

of charged particles will be reviewed. Section II is devoted to the technological advances in the field of high average power femtosecond laser systems operating at hundreds of kHz and MHz repetition rates; in particular, fiber-based chirped pulse amplification (CPA) systems will be discussed as they represent one of the most promising approaches for the generation of isolated attosecond pulses up to the MHz repetition rate. In this context, issues regarding the control of the electric field waveform and the stabilization of the carrier-envelope phase (CEP) will be analyzed; alternative approaches based on CEP tagging of a single laser pulse will be discussed. The latest advances for the characterization of isolated attosecond pulses (and more general attosecond waveforms) will be discussed with emphasis on the problems connected to the measurement of pulses close to the atomic unit of time. Finally, a brief overview of electron and ion spectrometers used in combination with attosecond XUV sources will be presented. In Section III, the attention will be focused on experiments performed on helium using train or isolated attosecond pulses; in particular, the potentialities of a complete characterization of the momentum of charged particles for a complete understanding of attosecond dynamics will be illustrated.

II. Technology

A. Harmonic Generation at High Repetition Rates

Isolated attosecond pulses can be generated with energies typically in the picojoule range at a repetition rate of few kHz. These two aspects have limited so far the application of such pulses for time-resolved investigations for two different reasons. The low energy of the isolated attosecond pulses, in combination with the low cross section for multiphoton processes in the XUV region, has prevented the implementation of purely attosecond pump–probe experiments. Nonlinear processes in the XUV region have been observed and used to characterize the pulse duration of trains of attosecond pulses using multi-mJ pump lasers [11], [12], and for Fourier-resolved XUV spectroscopy [13], [14] (for a review on multiphoton processes induced by high-order harmonics, see [15]). However, in spite of the intrinsic low-conversion efficiency associated with the high-order harmonic generation (HHG) process, for several applications the XUV fluxes, which can be achieved with currently available multi-mJ systems, do not represent the limiting factor. We can consider a typical coincidence measurement of charged particles, i.e., an experiment measuring electrons and ions emerging from an atom or molecule after absorption of an XUV photon and estimate the number of events expected considering typical experimental conditions. The typical target density that can be achieved in a cold atomic or molecular beam is on the order of $\rho = 10^{11}$–10^{12} cm^{-3} with a target extension of $L = 1$ mm [16]. The XUV photon flux can strongly depend on the driving pulse energy, pulse duration, and focusing condition; nowadays, isolated attosecond pulses with a number of photons $N_{\rm ph} = 4 \times 10^7$ can be achieved [1]. Taking into account that total cross sections around 50 nm are in the range of $\sigma = 1$–100 Mb (1 Mb $= 10^{-22}$ m^2) for noble gases [17], the total number of events N can be determined as

$$N = \rho L \sigma N_{\rm ph} = 0.4 - 400. \quad (1)$$

Such conditions are well suited for coincidence measurements that usually require less than one event per laser shot in order to univocally assign to the same reaction the measured particles. The main limitation for such experiments turns out to be that either the density of the target is much lower than the one considered (as for example in the case of dimers or clusters of noble gases that can be generated in a cold supersonic beam but only in a small percentage with respect to the background of monomers), or the reaction channel under investigation is characterized by a cross section that is considerably smaller than the total cross section at the excitation energy of interest. In all these cases, a key improvement would be the possibility to acquire data at a higher repetition rate and to sort them out according to particular conditions.

Several approaches for the generation of high-order harmonics at high repetition rates have been experimentally investigated over the past years. Using a 100 kHz repetition rate amplified laser system delivering 7 μJ per pulse and optimized focusing conditions, high harmonics (up to the 45th) were observed in xenon [18]. Recently phase matched HHG using a 25 μJ, 50 kHz titanium:sapphire (Ti:Sa) based laser system was demonstrated [19]. A different approach relies on the coherent buildup of pulses delivered at the MHz repetition rate by a laser cavity in order to reach the intensity required for efficient harmonic generation. The coherent buildup of the pulses was realized using an enhanced cavity whose modes were adjusted using feedbacks loops to match the laser modes of the main cavity. Inside the second cavity, the pulses were focused in a xenon gas jet for generation of XUV radiation that was extracted outside the cavity by means of a sapphire plate. Harmonics up to the 13th-order were observed up to several MHz repetition rate and will be applied for experiments requiring frequency combs in the XUV range [20]–[22]. Extension of such techniques for the generation of isolated attosecond pulses, that usually requires few cycle or short driving pulses ($<$30 fs), however, poses several challenges to the time duration of the driving pulse circulating in the enhanced cavity. Finally, harmonic generation at MHz repetition rate was demonstrated using directly the output of a femtosecond oscillator by using nanostructures to enhance the conversion efficiency of the process [23].

Due to the intrinsic rather low energy of the driving pulses achievable with conventional laser amplifiers, femtosecond oscillators, or enhanced cavities, in the past years different technological approaches have been developed in order to reach the average power levels required for HHG and single attosecond production at high repetition rate. One of the main aspects that has to be considered is the management of the thermal load inside the active material (typically solid state material such as Ti:Sa). Cryogenic cooling is as a very effective method for reaching final output powers up to tens of watts; this method, indeed, allows efficient heat extraction from the laser material reducing unwanted thermal effects such as thermal lensing. Systems with a repetition rate up to a few tens of kHz and energies of a few mJ are nowadays commercially available.

Another possibility to reduce unwanted thermal effects is the use of a long gain medium to spread the absorption of the pumping energy over a rather long distance and reduce the concentration of heat load; this is the main concept behind CPA fiber-based laser systems that can deliver output powers approaching 1 kW, at a repetition rate of 78 MHz and pulse durations of several hundreds of femtoseconds [24]. Pulses delivered by a similar source have been directly used for harmonic generation [25], or have been used as a pump for an optical parametric amplifier (OPA) [26]. Due to the large gain bandwidth, schemes for the generation of few-cycle pulses in Optical Parametric Chirped Pulse Amplification (OPCPA) systems have been already produced [27], [28]; moreover, first results clearly indicate that using CEP controlled input pulses, the phase stability is preserved in the amplification process [27]. All these characteristics make fiber-pumped few-cycle OPCPA an ideal tool for generation of isolated attosecond pulses at high repetition rates.

B. CEP Stabilization

The control of the CEP is a key point for the generation of isolated attosecond pulses. It is important to note that, even though the first characterization of a sub-fs pulse with a duration of 650 as was performed using a non CEP-stable driving few-cycle laser [29], reliable generation of isolated attosecond pulses has greatly benefited from the possibility of controlling the CEP of high peak intensity laser amplifiers [30]. The use of high repetition rate laser systems will require the development of faster feedback loops for the control of the CEP fluctuations. The loops developed so far contain moving mechanical parts that limit their bandwidths to few Hertz. Recently a new approach based on the use of a programmable acousto-optic dispersive filter (DAZZLER) was proposed [31]. In combination with methods for the fast, single shot detection of the CEP value or of the CEP drift based on Above Threshold Ionization (ATI) [32] or on nonlinear interferometers [33], DAZZLER-based feedback loops with bandwidths up to several tens of kHz should be feasible. The fast, single-shot detection techniques open, at the same time, the possibility to tag each laser pulse with the corresponding CEP offering an alternative way to perform attosecond experiments (and more general CEP-dependent investigations) without the need to stabilize the CEP. This approach could be useful for those experiments requiring the analysis of the response of a system to different CEPs of the driving infrared (IR) field.

It is interesting to observe that recently, using the Generalized Double Optical Gating (GDOG) technique [34], it has been shown that isolated attosecond pulses can be generated by using non CEP-stable driving pulses [35]. The GDOD technique is based on the use of two pulses of duration τ_p with counterrotating circular or elliptical polarization (ellipticity ε) that propagate collinearly with a temporal delay T_d. Only in the central part, where the two pulses have similar amplitude the total polarization is linear; outside this time window the polarization of the overall pulse is elliptical. In addition a rather weak second harmonic field is present in order to break the inversion symmetry of the total field increasing the duration of the time window for generation of a single attosecond pulse. As the HHG is extremely sensitive to the polarization ellipticity of the driving pulse (an ellipticity of $\varepsilon = 0.13$ determines a reduction of a factor 2 of the harmonic yield with respect to the linear polarization case [36]), generation of XUV radiation is possible only in the central temporal window, whose duration δt_g can be estimated as [37]:

$$\delta t_g = \frac{\varepsilon \tau_p^2}{(\ln 2) T_d} \tag{2}$$

If the condition $\delta t_g < T_0$ (where T_0 is the oscillation period of the driving fundamental field) is verified, only a single electron trajectory (ionization, acceleration and recombination) is present inside the temporal gate. As the CEP is varied, this path moves towards the edges of the gate determining a reduction of the harmonic yield; the harmonic spectrum, however, remains continuous for all CEPs. Experimental evidences were obtained by generating XUV continua for different CEPs and characterizing their temporal structure in a cross-correlation experiment between the XUV pulse and a synchronized replica of the IR pulse. The results are shown in Fig. 1, which reports the photoelectron distributions measured for four CEPs of the driving pulse. The variation of the signal, upon changing the CEP, depends on the position of the electron trajectory inside the gate; for all phases, the cross-correlation presents oscillations, typical of an isolated attosecond pulse. It must be observed, however, that in such conditions the intensity of the attosecond pulse strongly depends on the CEP of the driving field.

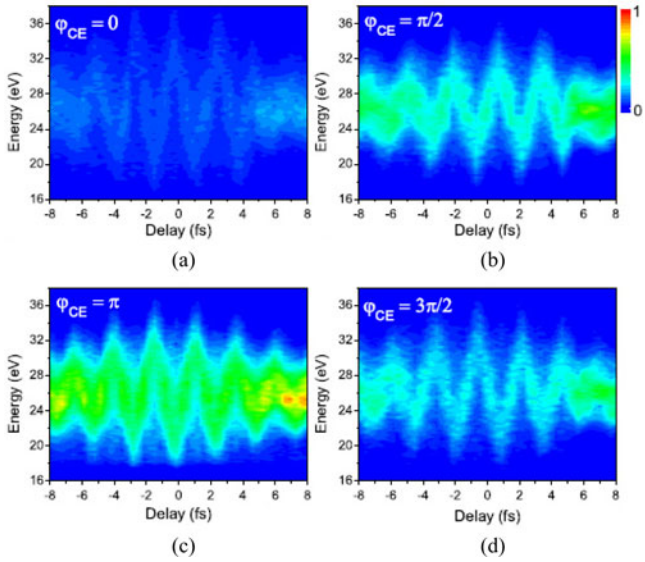

Fig. 1. Measured photoelectron energy distributions as a function of the delay between the XUV pulse, generated using the GDOD technique, and a synchronized CEP-stabilized IR pulse for four different CEPs (φ_{CE}): (a) $\varphi_{CE} = 0$, (b) $\varphi_{CE} = \pi/2$, (c) $\varphi_{CE} = \pi$, (d) $\varphi_{CE} = 3\pi/2$. Reprinted with permission from [34]. Copyright (2010) by the American Physical Society.

C. Characterization of Attosecond Pulses

A complete characterization of attosecond pulses is fundamental for further developments in the generation of shorter

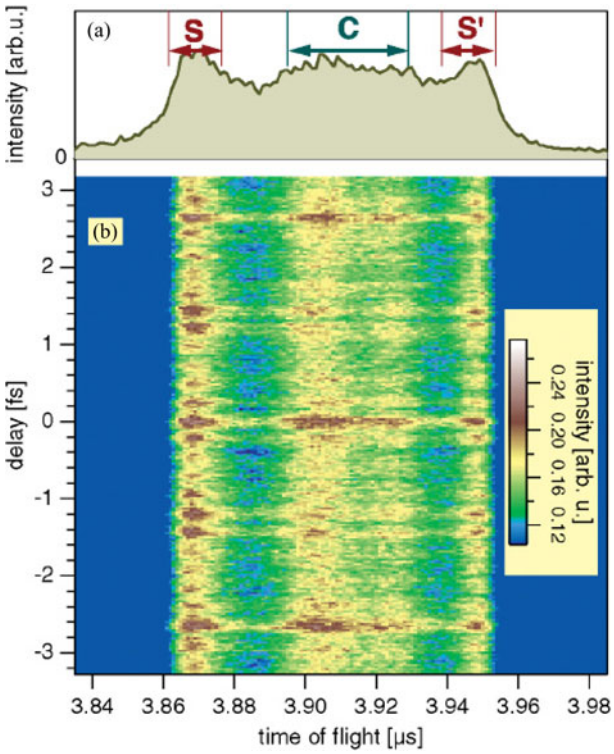

Fig. 2. Measured time of flight of ions released by two-photon absorption as a function of the delay between the two XUV attosecond pulse trains (b). Ion signal integrated over the delay scan. The bands *S* and *S'* can be attributed to the N^+ ion; different ion species and ionization pathways contribute to the region C (a). Reprinted with permission from [12]. Copyright (2006) by the American Physical Society.

pulses or with controllable waveforms. For several applications, such as transient absorption spectroscopy [38]–[40] or wave-packet interferometry [41], multiple attosecond pulses, in particular pairs of attosecond pulses, are more desirable than isolated pulses. Complex attosecond waveforms can be achieved by a fine shaping of the polarization state of the driving pulse [42]. The extension to the attosecond regime of techniques for temporal characterization of femtosecond pulses has been so far only partly realized due to technological and physical limitations. Nonlinear techniques for the characterization of time structures in the XUV require extremely high intensities due to the low cross section for nonlinear effects in this energy range (for example, for two-photon double ionization in helium $\sigma \simeq 10^{-53}$ cm^4 s [43]) with respect to the visible and near IR spectral region. XUV nonlinear effects have been observed with intensity as low as $I = 10^{11}$ W/cm^2 [44]. Two-photon single ionization of atoms (helium) or molecules (N_2) was used to characterize trains of attosecond pulses [11], [45], [46]. In this case higher XUV intensities in the order of $I = 10^{13}$–10^{14} W/cm^2 were reached by using high energy driving pulses (multi-mJ) and loose focusing geometry to increase the focal volume for harmonic generation. Fig. 2 shows the measured N^+ ion signal measured after Coulomb explosion of the molecular ion N_2^{+2} created by two-photon absorption. The XUV field was the combination of two trains of attosecond pulses with a variable delay τ. The oscillation of the signal as a function of the delay clearly indicates a dependence on the relative delay between the two fields; the total ion signal depends quadratically on the intensity of the XUV field (not shown), indicating the absorption of two XUV photons as the origin of the process leading to the formation of N^+ ion. The trace in Fig. 2 represents an interferometric autocorrelation of the train of attosecond pulses, from which important properties of the pulses inside the train, such as the π phase difference between consecutive pulses, can be extracted.

Nonlinear techniques cannot be immediately extended to the characterization of isolated attosecond pulses due to their considerably lower energy content. In general, a complete characterization of a light pulse can be accomplished in the frequency domain by measuring the spectral intensity $I(\omega)$ and the spectral phase $\varphi(\omega)$. Whereas the measurement of the spectral intensity can be performed by using an XUV spectrometer, the measurement of the spectral phase is more involved and requires a complex approach. Cross-correlation methods based on the measurement of the electrons photoionized by the XUV in the presence of an IR field have been mainly used for the temporal characterization of single attosecond pulses. The basic principle of the measurement can be understood in terms of classical mechanics: the attosecond pulse ionizes at an instant t' the atoms of a gas jet in the presence of a strong field, and imprints its temporal phase $\varphi(t')$ on the kinetic energy E_k of the emitted electrons according to the relation (in atomic units):

$$E_k(t') = \frac{1}{2}\mathbf{v}^2(t') = \omega(t') - I_p \tag{3}$$

where $\omega(t') = d\varphi(t')/dt'$ is the instantaneous frequency of the XUV pulse, $\mathbf{v}(t')$ is the electron initial velocity and I_p is the ionization potential of the atom. Therefore, the electron is freed with an energy that depends on the release instant t'. After ionization, the electrons are accelerated by the external electric field of the IR pulse and end up with a kinetic energy given by

$$E_k(t \to +\infty) = \frac{1}{2}[\mathbf{v}(t') + \mathbf{A}(t';\tau)]^2 = \frac{1}{2}\mathbf{p}^2 \tag{4}$$

where $\mathbf{A}(t';\tau)$ indicates the vector potential of the IR field delayed by τ with respect to the XUV field, and $\mathbf{p} = \mathbf{v} + \mathbf{A}$ is the electron momentum.

In terms of the electron wave packet the probability for ionization at an instant t' by the XUV pulse is given by

$$\mathbf{d}_{\mathbf{v}(t')} \cdot \mathbf{E}_{XUV}(t') \tag{5}$$

where $\mathbf{d}_{\mathbf{v}(t')}$ is the matrix element for a transition from the bound state (usually the ground state) to a continuum state with momentum $\mathbf{p} = \mathbf{v}(t') + \mathbf{A}(t')$ in the dipole approximation. It is important to observe that under the assumption that the matrix dipole moment does not considerably vary (in phase and amplitude) over the energy range covered by the attosecond pulse bandwidth, the electron wave packet is a replica of the attosecond pulse. This condition is not always met, as for example in presence of Cooper minima [47]. The vector potential will modulate in time the phase of the electron wave packet through

the term $\exp[i\Phi(t)]$ given by [48]:

$$\Phi(t) = -\int_{t}^{+\infty} dt''[\mathbf{v}\cdot\mathbf{A}(t'') + \mathbf{A}^2(t'')/2]$$
$$= -\int_{t}^{+\infty} dt'' U_p(t'') + \frac{\sqrt{8WU_p}}{\omega_L}\cos\theta\cos\omega_L t$$
$$- (U_p/2\omega_L)\sin 2\omega_L t \quad (6)$$

where ω_L is the frequency of the IR field, U_p is the ponderomotive potential of the IR, θ is the angle between the velocity $\mathbf{v}$ and the vector potential $\mathbf{A}$ and $W = \mathrm{p}^2/2$ is the final kinetic energy of the electron. The modulation of the temporal phase corresponds to a shift of the energy components of the electron wave packet; in particular, the IR field affects the width and the peak value of the photoelectron distribution. This technique is usually referred to as attosecond streak camera [49], [50], because the IR field acts as a streaking field in analogy to electric fields varying on the nanosecond or microsecond timescale that are used to characterize electrical signals in time. By measuring the streaking effect on the photoelectron distribution for different time delays, pulses as short as 250 as were characterized in 2004 [51]. In 2005, Mairesse and Quére showed that the measured cross correlation trace can be regarded as a spectrogram of the XUV field according to the relation [48]

$$S(\omega,\tau) = \left|\int_{-\infty}^{+\infty} dt G(t)E(t-\tau)\exp(i\omega t)\right|^2 \quad (7)$$

where $G(t)$ is the so-called gate function and $E(t-\tau)$ is the electric field to be characterized. From such a spectrogram, complete characterization of the XUV electric field can be achieved using well-established inversion algorithms. This technique is well known in the femtosecond domain and is indicated as frequency resolved optical gating (FROG) [52]; its extension to the attosecond domain was dubbed as FROG-CRAB (FROG for Complete Reconstruction of Attosecond Bursts). In the case of the attosecond streak camera, the measured quantity is the distribution $a(\mathbf{p},\tau)$ of the photoelectrons for different time delays τ; such a distribution is described by the relation

$$a(\mathbf{p},\tau) = -i\int_{-\infty}^{+\infty} dt e^{i\Phi(t)}\mathbf{d}_{\mathbf{p}-\mathbf{A}(t)}\cdot\mathbf{E}_{XUV}(t-\tau)e^{i(W+I_p)t}, \quad (8)$$

The action of the IR pulse is that of a pure phase gate $G(t) = \exp[i\Phi(t)]$. Using algorithms such as the principal component generalized projections algorithm (PGPCA), it is possible to retrieve both the gate function and the electric field of the XUV pulse. However, it is fundamental to observe that even though the phase term $\Phi(t)$ depends on the energy W [see (6)], the FROG algorithms neglect such a dependence, considering an energy-independent phase modulation. This assumption is usually referred to as the central momentum approximation and it is well satisfied as long as the energy bandwidth does not exceed the central energy of the attosecond pulse. The FROG-CRAB technique has been applied so far for the characterization of isolated attosecond pulses generated by the polarization gating method [53], the cutoff selection by single-cycle driving pulses [1], the double optical gating, and GDOG [35]. However, XUV continua with bandwidths corresponding to the Fourier limit pulse duration close [4] or even below [5] the atomic unit of time, will require the development of new experimental approaches for temporal characterization.

In 2003, Quéré *et al.* proposed a technique based on the measurement of the photoelectron wave packet generated by two replicas of the same attosecond pulse and shifted in energy by an intense IR field [54]. The technique can be considered as an extension of the SPIDER (spectral phase interferometry for direct electric-field reconstruction) method [55] used in the femtosecond domain, where two replicas of the same pulse are delayed and shifted in frequency through sum-frequency generation in a nonlinear crystal using a strongly chirped visible-IR pulse. Simulations showed that the technique could be applied for the characterization of extremely short pulses down to 12.5 as. A similar approach was introduced in 2005 by Cormier *et al.*, analyzing the interferogram generated by two trains of attosecond pulses created by two delayed driving pulses slightly shifted in frequency [56]. From the interference pattern, observed either in the spectral domain (due to the time delay between the two driving pulses) or in the spatial domain when the two driving pulses are focused to slightly different positions [(in this case the technique has been dubbed SEA (spatially encoded arrangement) SPIDER], it is possible to reconstruct the time evolution of the train of attosecond pulses. Simulations indicate that such a technique could be also applied for the measurement of isolated attosecond pulses. Experimentally, it was implemented for the characterization of the 19th harmonic generated by a Ti:Sa laser amplifier [57]. The generation of two isolated attosecond pulses shifted in frequency and with a suitable delay, however, still represents a challenge from the experimental point of view.

Another approach was proposed by Dudovich and coworkers [58] that demonstrated *in situ* characterization of a train of attosecond pulses by adding a small second harmonic field to the fundamental field. Due to the symmetry breaking of the total driving field, even harmonics of the fundamental frequency were generated. By changing the delay between the two fields, their relative phase is varied inducing a modulation in the intensity of the even harmonics signal. By measuring such oscillation as a function of the delay, the relative phase of the odd harmonics can be characterized and the attosecond pulse train can be reconstructed. This approach could also be extended to the characterization of isolated attosecond pulses. Finally, in 2010, a new technique was proposed that could allow the characterization of broadband attosecond pulses using rather low intensity ($I = 10^{11}$ W/cm^2) IR fields. The method, indicated as PROOF (phase retrieval by omega oscillation filtering) [59] is closely related to the RABBITT (reconstruction of attosecond beating by interference of two-photon transitions) technique used for the characterization of trains of attosecond pulses [60]. In the RABBITT, the relative phase between two consecutive harmonics ω_{n+1} and ω_{n-1} is retrieved by measuring the photoelectron signal obtained by two-color (XUV+IR) photoionization. Two paths can contribute to the generation of electrons whose energy is intermediate between the photoelectron signal due to single photon absorption of the two harmonics: absorption of an XUV

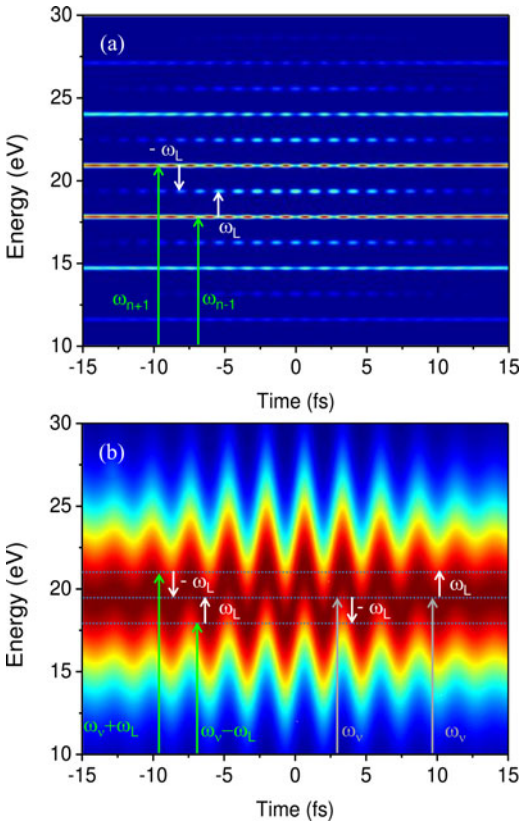

Fig. 3. (a) RABBITT method. Two paths contributing to the sideband signal of order n: absorption of a photon ω_{n+1} and emission of an IR photon ω_L; absorption of a photon ω_{n-1} and of a IR photon ω_L. (b) PROOF method. Four paths contributing to the signal at energy ω_v: the two paths on the left side are equivalent to the paths involved in a RABBITT measurement; the two paths on the right side correspond to the absorption of a photon energy ω_v and the absorption or emission of an IR photon ω_L, determining a reduction of the signal at ω_v.

photon of the harmonic $n+1$ and emission of an IR photon, or absorption of an XUV photon of the harmonic $n-1$ and of an IR photon [see Fig. 3(a)]. As the two paths are indistinguishable they interfere and the photoelectron signal (sideband of order n) presents a modulation given by [61], [62]:

$$A_f \cos(2\varphi_L + \varphi_{n-1} - \varphi_{n+1} + \Delta\varphi^f_{\text{atomic}}) \quad (9)$$

where the term A_f depends on the matrix dipole moments between the initial and final states, $(\varphi_{n-1} - \varphi_{n+1})$ is the difference between the phases of the harmonics $n+1$ and $n-1$, $2\varphi_L$ represents the phase term associated with the IR field and $\Delta\varphi^f_{\text{atomic}}$ is the phase difference of the matrix elements corresponding to photoionization from the $n+1$ and $n-1$ harmonics. The physical interpretation of the PROOF technique is closely related to the previous formula but takes into account that the XUV spectrum is no longer a discrete series of harmonics but a continuum distribution [see Fig. 3(b)]. The photoelectron signal at energy ω_v is due to the superposition of three terms oscillating at different frequencies:

$$I(\omega_v, \tau) = I_0 + I_{\omega_L} + I_{2\omega_L}. \quad (10)$$

The three terms on the right-hand side of (10) represent a constant term (I_0) and two terms oscillating in time with frequency ω_L (I_{ω_L}) and $2\omega_L$ ($I_{2\omega_L}$), respectively. From the term oscillating at the IR frequency ω_L, it is possible to extract the phase of the attosecond pulse. Indeed, this term is given by four different contributions:

$$\begin{aligned} I_{\omega_L} \propto & -U(\omega_v)U(\omega_v+\omega_L)e^{i[\varphi(\omega_v)-\varphi(\omega_v+\omega_L)]}e^{(i\omega_L\tau)} \\ & + U(\omega_v)U(\omega_v+\omega_L)e^{i[\varphi(\omega_v+\omega_L)-\varphi(\omega_v)]}e^{(-i\omega_L\tau)} \\ & + U(\omega_v)U(\omega_v-\omega_L)e^{i[\varphi(\omega_v)-\varphi(\omega_v-\omega_L)]}e^{(-i\omega_L\tau)} \\ & - U(\omega_v)U(\omega_v-\omega_L)e^{i[\varphi(\omega_v-\omega_L)-\varphi(\omega_v)]}e^{(i\omega_L\tau)} \end{aligned} \quad (11)$$

where $U(\omega)$ and $\varphi(\omega)$ are the spectral amplitude and phase of the XUV pulse at frequency ω, respectively. The first term of (11) represents a final state with energy $\omega_v + \omega_L$ that can be reached either by direct photoabsorption of a photon $\omega_v + \omega_L$ or by the absorption on an XUV photon ω_v and an IR photon ω_L. These two terms interfere depending on the relative phase of the two paths: $\varphi(\omega_v) - \varphi(\omega_v + \omega_L) + \omega_L\tau$. The second term represents a final state with energy ω_v that can be reached by direct absorption of an XUV photon ω_v or by a two-color process: absorption of an XUV photon $\omega_v + \omega_L$ and emission of an IR photon ω_L. This term will contribute to the signal at frequency ω_v. The third term corresponds to a signal at frequency $\omega_v - \omega_L$, and the fourth one to a signal at frequency ω_v involving absorption of a photon $\omega_v - \omega_L$. It is important to observe that this interpretation is closely related to the interpretation of the RABBITT signal the main difference being that in the case of the RABBITT no XUV photon at the harmonic n is present as the XUV spectrum is composed of a discrete series of odd harmonics. In the RABBITT and PROOF techniques, the intensity of the IR fields should be limited to the perturbative regime as they rely on the assumption that only paths involving a single IR photon contribute to the signal. Upon increasing the IR intensity, this assumption becomes invalid and systematic error can be introduced in the reconstruction of the attosecond field. However, also in such cases, simulations show that the PROOF method can reconstruct attosecond field waveforms with a precision superior to the FROG-CRAB technique [59].

D. Characterization of Attosecond Dynamics

Isolated attosecond pulses generated so far have a central energy in the XUV range between 20 eV [63] and 100 eV [1]. When such pulses are focused on a medium they will lead to the emission of a photoelectron wave packet; the release of one (or more) electron, in general, leaves the ionized system in a nonstationary state that will evolve in time with a dynamics that can take different forms depending on the original target. The measurement of the charged particles involved in the process allows one to elucidate not only the photoionization initial step but also the pathway followed in the subsequent reaction. In general, the more accurate the characterization is, the more detailed the information about the dynamics are. Therefore, a complete characterization of the angular and energy distributions is helpful in distinguishing the contributions of different reaction channels. Moreover, measurements in coincidence of

ions and electrons allow to retrieve information about physical and chemical mechanisms in the molecular frame.

Velocity map imaging (VMI) spectrometers are suitable devices for measuring the angular and energy distributions of both ions and electrons [64]. An iterative inversion procedure can be used to reconstruct the 3-D momentum distributions of the emitted particles starting from its 2-D projection on the detector [65]. VMI spectrometers are suited for studying photoionization dynamics of atoms and molecules in the laboratory frame, e.g., they have been implemented to measure electron localization in D_2 molecules induced by few-cycle CEP stabilized laser pulses [66] and to study impulsive alignment and orientation of molecules [67], [68]. In this context, major efforts for increasing the number of events per pulse have been invested, focusing on optimized design of the gas injection system [69] and a newly designed detector for the replacement of microchannel plates detectors that represents one of the main limiting factors concerning the gas density in the interaction region [70]. Combination of a VMI spectrometer with techniques for impulsive alignment and orientation of molecular systems [71] will allow measurements of photoelectron distributions in the molecular frame.

Reaction microscopes (REMIs) [16] are spectrometers suited for the study of electron correlations. Indeed, they allow to perform kinematically complete experiments in which the momentum of all charge particles involved in a physical or chemical reaction are measured. Such characteristics allow one to study reaction channels characterized by low cross sections that could not be investigated otherwise. So far they have been largely used with synchrotron-based XUV radiation to investigate the response of molecules or atoms to XUV or X-ray photons. They have been implemented for the investigation of interatomic Coulombic decay [72], an important relaxation process in hydrogen bonded [73], [74], and van der Waals clusters [75]. Only a few experiments have been reported so far showing the use of HHG-based XUV radiation and REMIs [76], [77]. The implementation of such techniques in combination with isolated attosecond pulses presents new challenges mainly due to the average photon flux and to the density of the species to be investigated. Indeed, in order to obtain high-momentum resolution, REMIs usually use supersonic gas-jets for the generation of cold atomic or molecular beams as a target source, because the recoil momentum of the ion is comparable with the initial velocity spread at room temperature. They are based on the expansion in vacuum of high-pressure gases through a small aperture; a well-defined beam is then obtained by placing a suitable number of apertures in the beam path. Typically, densities on the order of 10^{11}–10^{12} cm^{-3} can be achieved. However, only a limited number of atomic and molecular species can be efficiently cooled in such a way (e.g., noble gases and small molecules such as CO_2, H_2, N_2, and O_2). Larger molecules, such as biomolecules that at room temperature are not in the gas phase, cannot be efficiently cooled using this approach. Investigation of such molecules on the sub-fs timescale could offer new perspectives as theoretical predictions have shown that electron correlations can drive important charge rearrangement processes (charge migration) on the ultrashort timescale after photoionization from an inner-valence shell [78], [79]. Expansion using a buffer gas (typically helium) could be implemented to put into the gas phase a large variety of complex molecules at the expense of a lower target density. Another issue related to the use of complex molecules is the presence of different conformers that will require additional effort for the target preparation. Sub-fs charge migration can be strongly influenced by the structure of the molecules, indeed, and occur on different timescales depending on the particular conformer [80]. Selection of a single conformer will be required for investigation on a well defined and prepared target sample. Recently, experimental techniques have been demonstrated for the separation of different conformers species exploiting the difference force induced by a static electric field on the rotational levels of a molecular sample [81]. This technique should offer the possibility to investigate a single conformer in a well-defined quantum state (ground rotational, vibrational, and electronic state).

III. Attosecond Science

Helium is a natural candidate for investigation of attosecond dynamics; in particular electron correlations can be ideally investigated in this system because of the simple electronic structure, and several theoretical works have analyzed the possibility to measure effects connected to the electron–electron interaction [82], [83]. Helium is also an ideal candidate for the investigation of Fano resonances [84], which are encountered in several physical problems. Theoretical works have shown that the time evolution of the photoelectron wave packets created in helium by an attosecond excitation centered around 60 eV could be characterized using intense [85] or rather moderate IR fields [86]. Its high-ionization threshold energy, moreover, allows one to investigate the dynamics of bound-state wave packets excited by ultrashort XUV radiation. In this section, we will review recent experiments in which attosecond pulses below and around the ionization threshold of helium have been used to elucidate and investigate different dynamics in the system. The section will be divided for convenience into two parts: the first one will be devoted to experiments realized using trains of attosecond pulses (or equivalently a discrete set of harmonics in the XUV range), while the second one will describe an experiment based on the application of an isolated attosecond pulse (corresponding to a continuum distribution).

A. Experiment in Helium by Trains of Attosecond Pulses

In 2007, Johnsson *et al.* reported on the control of the ionization probability of helium atoms by the combination of a train of attosecond pulses and an intense IR field [87]. The attosecond pulse train was composed by the superposition of the odd harmonics (from the 11th to the 17th) of a driving laser with wavelength of 800 nm (1.55 eV), characterized by a central energy below the ionization threshold. The attosecond pulse train and intense IR synchronized laser pulse were focused on a helium gas jet, and the delay between the two fields was varied with attosecond resolution, observing a strong modulation of the ionization probability (around 40%); such modulation was not observed in argon whose ionization threshold (15.79 eV) lies

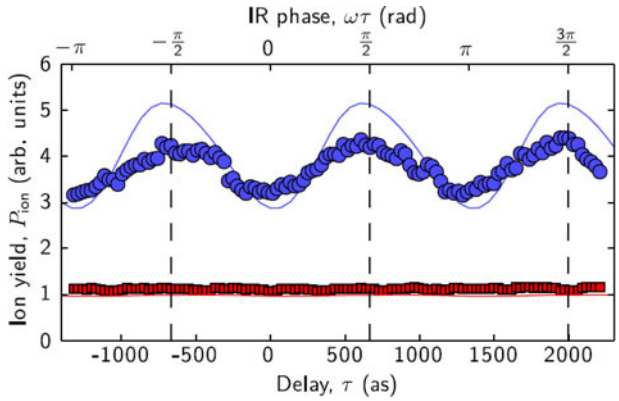

Fig. 4. Ion yield as a function of the relative delay between the attosecond pulse train and the IR field for helium (blue circles) and argon (red squares). Ionization probability obtained by solving the Schrödinger equation for the helium (blue line) and argon cases (red line). Reprinted with permission from [86]. Copyright (2007) by the American Physical Society.

well below the central energy of the harmonic comb, as shown in Fig. 4. The experimental results are in agreement with the solution of the time-dependent Schrödinger equation in the single active electron approximation [88]. The model reproduces the experimental data and allows one to interpret the modulation as the result of the interference among the wave packets created by the attosecond pulses in the train. In helium, the energy of a wave packet created by an attosecond pulse is so low that it will find itself still in the proximity of the parent ion when the subsequent wave packet is created half an optical cycle later. This condition gives rise to an interference effect that modulates the total ionization yield. In argon, this effect is not present due to the higher energy of the electron wave packet that will rapidly leave the parent ion.

A simple physical model to simulate the emission of the electron wave packet by a train of attosecond pulses was introduced by Riviére *et al*. using the strong field approximation (SFA) [89]. They derived a formula that describes the distribution of the momenta p for different relative phases φ between an attosecond pulse train lasting N IR cycles and the IR pulse:

$$\psi(\mathrm{p},\varphi) = \sum_{n=0}^{N-1} e^{2n\pi C}\left[e^{-iC\pi/2}\chi(\mathrm{p},\varphi) + e^{iC\pi/2}\chi(-\mathrm{p},\varphi)\right] \tag{12}$$

where $C = (\mathrm{p}^2/2 + U_p - \varepsilon_f)/\omega$ depends on the ponderomotive potential U_p and the energy $\varepsilon_f = I_p + \omega_{\mathrm{XUV}}$. The function $\chi(\mathrm{p},\varphi)$ describes the electron wave packet emitted by a single attosecond pulse. The observed photoelectron distribution will be given then by:

$$\begin{aligned}|\psi(\mathrm{p},\varphi)|^2 &= \left|\sum_{n=0}^{N-1} e^{2n\pi C}\right|^2 \left|\left[e^{-iC\pi/2}\chi(\mathrm{p},\varphi) + e^{iC\pi/2}\chi(-\mathrm{p},\varphi)\right]\right|^2 \\ &= \frac{\sin^2(N\pi C)}{\sin^2(\pi C)}\chi_2(\mathrm{p},\varphi) = K_N(\mathrm{p})\chi_2(\mathrm{p},\varphi).\end{aligned} \tag{13}$$

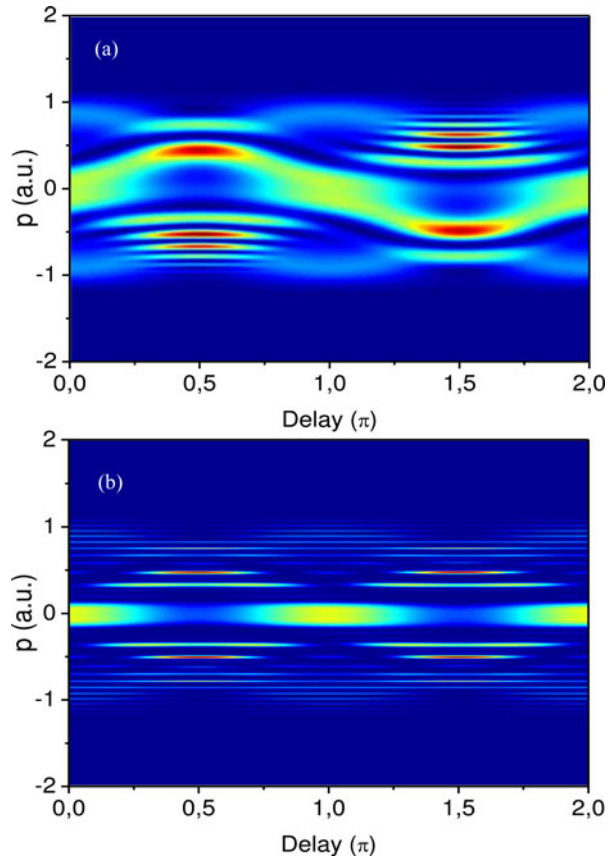

Fig. 5. (a) Electron wave packet $\chi_2(\mathrm{p},\varphi)$ emitted in a single IR cycle by two attosecond pulses. (b) Elecron wave packet emitted by a train of attosecond pulses according to (13). See [89].

The distribution can be, therefore, thought as the product of the function $K_N(\mathrm{p})$ taking into account the periodicity of the process due to the number of attosecond pulses, and the function $\chi_2(\mathrm{p},\varphi)$ that describes the photoelectron wave packet emitted in a single optical cycle [see Fig. 5(a)]. It must be observed that the function $K_N(\mathrm{p})$ does not depend on the phase between the IR and XUV pulse train, and that it acts as a filter on the wave packet emitted in a single cycle. The function $K_N(p)$ is characterized by sharp oscillating peaks that are not evenly spaced in momentum but that present a decreasing period as the momentum p increases. The product of the two terms, as shown in Fig. 5(b), corresponds to the electron wave packet emitted in the two-color process. The differences between the ion yield in helium and in argon are due to the fact that the wave packets emitted in a single cycle in the two cases are centered around different energies. The function $K_N(\mathrm{p})$, therefore, filters out different momentum regions that turns out to be characterized by an oscillation in the ion yield for different relative phases in the case of helium; on the other hand, in the case of argon, the relevant contribution, filtered out by the function $K_N(\mathrm{p})$ is centered at a different momentum and does not present an oscillation for different relative phases. This interpretation is consistent with the fact that, due to the low kinetic energy, the electron wave packet created in helium takes a longer time to leave the parent ion and can induce interference effects with the

wave packet ionized by the subsequent attosecond pulse. It is important to observe that excited atomic levels of helium could play an important role in the interpretation of the data reported in [87]. Indeed, as the experiments were performed using a set of sharp spectral peaks, a small detuning of the harmonics energy from the energy levels of the p states could strongly influence the behavior of the ionization probability as a function of the relative delay. This issue was carefully investigated in [90], measuring in coincidence the ion He^+ and the electron emitted. The authors used a set of three harmonics (13th–15th–17th) generated at two different driving wavelengths to study the ionization dynamics in the presence of an intense IR field. The use of a tunable driving laser for HHG is a powerful control tool as it allows to set one or more harmonics in resonance (or out of resonance) with respect to the p states. Using such an approach it was shown that the ionization probability presents a different qualitative evolution as a function of the relative delay depending on whether the harmonics are in or out of resonance. The theoretical analysis indicates that, additionally to the electron wave packet interference, the shift and broadening of the resonances due to the IR field can strongly influence the ionization probability. Such a statement was enforced by the analysis of the different angular momentum contribution to the total angular distribution of the emitted photoelectrons by below threshold harmonics; this analysis has showed that those harmonics, which are out of resonance without the IR field, can be made resonant with the atomic bound states by considering the dressing effect of the IR photons and can participate to the emission of photoelectrons. This observation can be explained considering that the intense IR field shifts the energy levels according to the instantaneous electric field and put into the resonance the harmonic, modulating on the cycle scale the ionization probability.

A tunable driving laser for the generation of tunable harmonic radiation was also used by Swoboda *et al*. to measure the phase of the resonant two-photon ionization process in helium [91]. The authors measured the electron sidebands generated by the combination of an IR field and by a comb of odd harmonics (15th–17th–19th–21st–23rd) below (15th) and above (all the others) the ionization threshold. In the RABBITT technique, the oscillation of the sidebands as a function of the relative phase between the IR and XUV field allows to retrieve the relative phase of the harmonics; in this case, the comparison of the sidebands generated by below (but resonant with the $1s3p$ state) and above ionization threshold harmonics, allows to eliminate the dependence on the phase properties of the harmonics and to retrieve the phase of the two-color ionization process for different IR intensities and different excitation energies.

B. Experiment in Helium by Isolated Attosecond Pulses

The typical XUV spectrum generated in xenon using a few-cycle pulse with time-dependent polarization is shown in Fig. 6; it presents components above and below the ionization threshold of helium. As the polarization gating technique is very efficient in the selection of a single electron path both in the plateau and in the cutoff region, by changing the generating gas, tunable XUV continua can be generated even at rather low central energies [92], [93]. Such XUV pulses were used in combination with a synchronized CEP-stable few-cycle pulse to perform a pump–probe experiment in helium [63]. The photoelectron spectra measured as a function of the delay between the two pulses in the upward direction (positive energy) and in the downward direction (negative energy) are shown in Fig. 7. They present oscillations with opposite phases as expected in the case of ionization with a subcycle XUV pulse. Upon increasing the delay between the IR and XUV pulses, the maximum energy shift diminishes and for positive delays ($\tau \geq 3$ fs), i.e., for the IR following the XUV pulse, and for low energies ($E \leq 3$ eV), a series of fringes whose spacing depends on the time delay, characterizes the photoelectron spectra. It is important to observe that such fringes are absent for negative time delays, i.e., when the IR pulse arrives before the XUV pulses. Their appearance indicates the existence of a process leading to photoionization by the IR and initiated by the XUV pulse. Indeed, the below-threshold components of the XUV spectrum, as shown in Fig. 6, can excite one electron to a p level by single photon absorption; at the same time the components above threshold can directly ionize the atom (see the schemes in Fig. 6). The wave packet created by the XUV pulse can be expressed in terms of eigenstates of the atomic Hamiltonian H_0 as

$$|\psi\rangle = \sum_n a_{np} e^{i\varphi_{np}} |np\rangle + \int d\mathbf{p}' a_{\mathbf{p}'} e^{i\varphi_{\mathbf{p}'}} |\mathbf{p}'\rangle \qquad (14)$$

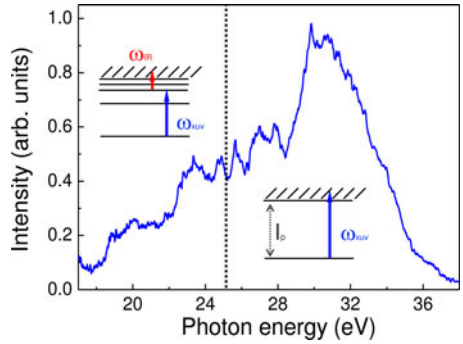

Fig. 6. XUV spectrum generated in xenon by CEP-stable few cycle pulse using the polarization gating technique. The black vertical line indicates the ionization threshold of helium; above threshold components can directly ionize helium, whereas below threshold components can excite one of the np states.

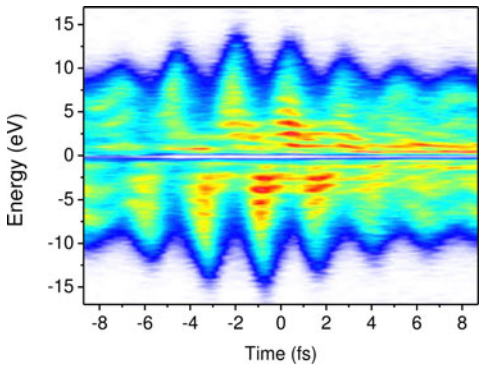

Fig. 7. Photoelectron spectra measured in helium as a function of the delay between the attosecond and IR pulse.

where a_{np} ($a_{\mathbf{p}'}$) and φ_{np} ($\varphi_{\mathbf{p}'}$) represent the initial amplitude and phase of the bound (continuum) state $|np\rangle$ ($|\mathbf{p}'\rangle$), respectively. The wave packet evolution is then controlled by the Hamiltonian $H = H_0 + \mathbf{r}\cdot\mathbf{E}_L$, including a dipole term taking into account the interaction with the IR field. It is important to point out that this schematization is only valid if the IR pulse arrives after the XUV pulse. The observation of an electron characterized by momentum $\mathbf{p}$ is then given by

$$M_{\mathbf{p}} = \langle \mathbf{p}|\psi(t)\rangle = \langle \mathbf{p}|U\psi\rangle \simeq \langle \mathbf{p}|U_L U_0 \psi\rangle \tag{15}$$

where U, U_0, and U_L represent the evolution operators associated to the total Hamiltonian H, the field free Hamiltonian H_0 and the dipole term $\mathbf{r}\cdot\mathbf{E}_L$, respectively. Following the approach developed in [94], it is possible to express the final transition to the state of momentum $\mathbf{p}$ as

$$\begin{aligned}|M_{\mathbf{p}}|^2 &= a_{\mathbf{p}^2} + \sum_{n} b_{\mathbf{p},np}^2 a_{np}^2 \\ &+ 2\sum_{n} a_{\mathbf{p}} b_{\mathbf{p},np} a_{np} \cos[\Phi_{\mathbf{p},np} - (\varepsilon_{\mathbf{p}} - \varepsilon_{np})\tau] \\ &+ 2\sum_{n<m} b_{\mathbf{p},np} b_{\mathbf{p},mp} a_{np} a_{mp} \cos[\Phi_{mp,np} - (\varepsilon_{mp} - \varepsilon_{np})\tau]\end{aligned} \tag{16}$$

where the term $\Phi_{\mathbf{p},np}$ contains the terms due the Volkov phase and the dipole phases involved in the transition from the ground state to the continuum $|\mathbf{p}\rangle$ and in transition first from the ground state to the bound state $|np\rangle$ and then to the continuum $|\mathbf{p}\rangle$. Similarly, the phase $\Phi_{mp,np}$ is related to the phase difference between the path from the ground state to the continuum $|\mathbf{p}\rangle$, through the bound state $|mp\rangle$ and $|np\rangle$. The coefficient $b_{\mathbf{p},np}$ are the amplitude of the matrix elements associated with the transitions among the states $|np\rangle$ and $|\mathbf{p}\rangle$. Finally, $\varepsilon_{np,mp}$ and $\varepsilon_{\mathbf{p}}$ indicate the energies of the bound states $|np\rangle$, $|mp\rangle$ and of the continuum state $|\mathbf{p}\rangle$, respectively.

The first and second term on the right-hand side of (16) correspond to direction ionization to the p states by the XUV and ionization by the combination of the IR and XUV field, respectively. The third term corresponds to an interference term between a direct ionization to a $\mathbf{p}$ state and ionization by the IR field of a bound state $|np\rangle$ excited by the XUV pulse. Finally, the fourth term corresponds to the interference between two bound states excited by the XUV ($|np\rangle$ and $|mp\rangle$) and ionized by the IR field. The two distinct interference patterns are characterized by a different evolution as a function of the delay τ and of the observation energy $\varepsilon_{\mathbf{p}}$. Indeed, (16) indicates that the equiphase surfaces in the (τ, ε) plane are given for the third term by the relation:

$$\cos[\Phi_{\mathbf{p},np} - (\varepsilon_{\mathbf{p}} - \varepsilon_{np})\tau] = \text{const.} \Rightarrow \tau \propto 1/(\varepsilon_{\mathbf{p}} - \varepsilon_{np}) \tag{17}$$

and are represented by hyperbola. The onset of such lines can be recognized in Fig. 7 at low energies and for positive time delays. The dependence on the delay and energy is more evident by considering the evolution of the interference fringes on an extended time interval [see 63, Fig. 2]. For the fourth term of (16), the corresponding relation is

$$\cos[\Phi_{mp,np} - (\varepsilon_{mp} - \varepsilon_{np})\tau] = \text{const.} \Rightarrow \tau \propto 1/(\varepsilon_{mp} - \varepsilon_{np}). \tag{18}$$

These surfaces do not depend on the energy $\varepsilon_{\mathbf{p}}$ and are represented by lines parallel to the energy axes and can be recognized for longer time delays [not visible in Fig. 7; see 63, Fig. 4(e)]. It is important to observe that the characterization of the angular distribution of the photoelectrons allows to distinguish between the two interference terms. Indeed, the two ionization channels are characterized by the absorption of a different number of photons: the direct channel involves the absorption of a single XUV photon leading to the emission of an electron in a p ($l = 1$) state; on the other hand, the indirect channel requires the absorption of one XUV photon and one IR photon (or more depending on the IR intensity), leading to emission of an electron in an s ($l = 0$) or d state ($l = 2$). Applying a decomposition in Legendre polynomials of the measured angular distribution, the different contributions can be separated, as shown in [63, Fig. 4] .

IV. Conclusion

Several main advances in the field of attosecond technology have been reviewed, focusing the attention on the experimental setups for the generation and characterization of attosecond pulses approaching the atomic unit of time at hundreds of kHz and even MHz repetition rates. The availability of such sources of coherent ultrashort XUV radiation will open new opportunities for the investigation of kinematically complete experiments in which electrons and ions are measured in coincidence for a complete reconstruction of atomic and molecular reactions. First experiment on helium indicates that the measurement of the angular distribution of photoelectron wave packets allows to characterize in more detail photoionization processes modified by an intense IR field or involving more than one ionization channel.

Acknowledgment

The authors would like to thank P. Riviére, J. Mauritsson, and M. Vrakking for stimulating discussions.

References

[1] E. Goulielmakis, M. Schultze, M. Hofstetter, V. Yakovlev, J. Gagnon, M. Uiberacker, A. L. Aquila, E. M. Gullikson, D. T. Attwood, R. Kienberger, F. Krausz, and U. Kleineberg, "Single-cycle nonlinear optics," *Science*, vol. 320, no. 5883, pp. 1614–1617, 2008.

[2] T. Brabec and F. Krausz, "Intense few-cycle laser fields: Frontiers of nonlinear optics," *Rev. Mod. Phys.*, vol. 72, no. 2, pp. 545–591, 2000.

[3] M. B. Gaarde, J. L. Tate, and K. J Schafer, "Macroscopic aspects of attosecond pulse generation," *J. Phys. B: At. Mol. Opt. Phys.*, vol. 41, no. 13, p. 132001, 2008.

[4] G. Sansone, F. Ferrari, C. Vozzi, F. Calegari, S. Stagira, and M. Nisoli, "Towards atomic unit pulse duration by polarization-controlled few-cycle pulses," *J. Phys. B: At. Mol. Opt. Phys.*, vol. 42, no. 13, p. 134005, 2009.

[5] H. Mashiko, S. Gilbertson, M. Chini, X. Feng, C. Yun, H. Wang, S. D. Khan, S. Chen, and Z. Chang, "Extreme ultraviolet supercontinua supporting pulse durations of less than one atomic unit of time," *Opt. Lett.*, vol. 34, no. 21, pp. 3337–3339, 2009.

[6] M. Drescher, M. Hentschel, R. Kienberger, M. Uiberacker, V. Yakovlev, A. Scrinzi, Th. Westerwalbesloh, U. Kleineberg, U. Heinzmann, and

F. Krausz, "Time-resolved atomic inner-shell spectroscopy," *Nature*, vol. 419, no. 6909, pp. 803–807, 2002.

[7] G. Sansone, F. Kelkensberg, J. F Pérez-Torres, F. Morales, M. F. Kling, W. Siu, O. Ghafur, P. Johnsson, M. Swoboda, E. Benedetti, F. Ferrari, F. Lépine, J. L Sanz-Vicario, S. Zherebtsov, I. Znakovskaya, A. L'Huillier, M. Y. Ivanov, M. Nisoli, F. Martín, and M. J. J. Vrakking, "Electron localization following attosecond molecular photoionization," *Nature*, vol. 465, no. 7299, pp. 763–767, 2010.

[8] A. L. Cavalieri, N. Müller, Th. Uphues, V. S. Yakovlev, A. Baltuška, B. Horvath, B. Schmidt, L. Blümel, R. Holzwarth, S. Hendel, M. Drescher, U. Kleineberg, P. M. Echenique, R. Kienberger, F. Krausz, and U. Heinzmann, "Attosecond spectroscopy in condensed matter," *Nature*, vol. 449, no. 7165, pp. 1029–1032, 2007.

[9] E. Goulielmakis, Z.-H. Loh, A. Wirth, R. Santra, N. Rohringer, V. S. Yakovlev, S. Zherebtsov, T. Pfeifer, A. M. Azzeer, M. F. Kling, S. R. Leone, and F. Krausz, "Real-time observation of valence electron motion," *Nature*, vol. 466, no. 7307, pp. 739–743, 2010.

[10] H. Wang, M. Chini, S. Chen, C.-H. Zhang, F. He, Y. Cheng, Y. Wu, U. Thumm, and Z. Chang, "Attosecond time-resolved autoionization of argon," *Phys. Rev. Lett.*, vol. 105, no. 14, p. 143002, 2010.

[11] Y. Nabekawa, T. Shimizu, Y. Furusawa, E. J. Takahashi, and K. Midorikawa, "Interferometry of attosecond pulse trains in the extreme ultraviolet wavelength region," *Phys. Rev. Lett.*, vol. 102, no. 21, p. 213904, 2009.

[12] Y. Nabekawa, T. Shimizu, T. Okino, K. Furusawa, H. Hasegawa, K. Yamanouchi, and K. Midorikawa, "Interferometric autocorrelation of an attosecond pulse train in the single-cycle regime," *Phys. Rev. Lett.*, vol. 97, no. 15, p. 153904, 2006.

[13] T. Okino, K. Yamanouchi, T. Shimizu, R. Ma, Y. Nabekawa, and K. Midorikawa, "Attosecond nonlinear Fourier transformation spectroscopy of CO_2 in extreme ultraviolet wavelength region," *J. Chem. Phys.*, vol. 129, no. 16, p. 161103, 2008.

[14] Y. Furukawa, Y. Nabekawa, T. Okino, S. Saugout, K. Yamanouchi, and K. Midorikawa, "Nonlinear Fourier-transform spectroscopy of D_2 using high-order harmonic radiation," *Phys. Rev. A*, vol. 82, no. 1, p. 013421, 2010.

[15] K. Midorikawa, Y. Nabekawa, and A. Suda, "XUV multiphoton processes with intense high-order harmonics," *Progr. Quant. Electron.*, vol. 32, no. 2, pp. 43–88, 2008.

[16] J. Ullrich, R. Moshammer, A. Dorn, R. Dörner, L. Ph. H. Schmidt, and H. Schmidt-Böcking, "Recoil-ion and electron momentum spectroscopy: Reaction-microscopes," *Rep. Prog. Phys.*, vol. 66, no. 9, p. 1463, 2003.

[17] J. B. West and G. V. Marr, "The absolute photoionization cross sections of helium, neon, argon and krypton in the extreme vacuum ultraviolet region of the spectrum," *Proc. R. Soc. Lond. A.*, vol. 349, no. 1658, pp. 397–421, 1976.

[18] F. Lindner, W. Stremme, M. G Schätzel, F. Grasbon, G. G. Paulus, H. Walther, R. Hartmann, and L. Strüder, "High-order harmonic generation at a repetition rate of 100 kHz," *Phys. Rev. A*, vol. 68, no. 1, p. 013814, 2003.

[19] M. C. Chen, M. R. Gerrity, S. Backus, T. Popmintchev, X. Zhou, P. Arpin, X. Zhang, H. C. Kapteyn, and M. M. Murnane, "Spatially coherent, phase matched, high-order harmonic EUV beams at 50 kHz," *Opt. Exp.*, vol. 17, no. 20, pp. 17376–17383, 2009.

[20] R. J. Jones, K. D. Moll, M. J. Thorpe, and J. Ye, "Phase-coherent frequency combs in the vacuum ultraviolet via high-harmonic generation inside a femtosecond enhancement cavity," *Phys. Rev. Lett.*, vol. 94, no. 19, p. 193201, 2005.

[21] C. Gohle, T. Udem, M. Herrmann, J. Rauschenberger, R. Holzwarth, H. A. Schuessler, F. Krausz, and T. W Hänsch, "A frequency comb in the extreme ultraviolet," *Nature*, vol. 436, no. 7048, pp. 234–237, 2005.

[22] A. Ozawa, J. Rauschenberger, Ch. Gohle, M. Herrmann, D. R. Walker, V. Pervak, A. Fernandez, R. Graf, A. Apolonski, R. Holzwarth, F. Krausz, T. W Hänsch, and Th. Udem, "High harmonic frequency combs for high resolution spectroscopy," *Phys. Rev. Lett.*, vol. 100, no. 25, p. 253901, 2008.

[23] S. Kim, J. Jin, Y.-J. Kim, I.-Y. Park, Y. Kim, and S.-W. Kim, "High-harmonic generation by resonant plasmon field enhancement," *Nature*, vol. 453, no. 7196, pp. 757–760, 2008.

[24] T. Eidam, S. Hanf, E. Seise, T. V. Andersen, T. Gabler, C. Wirth, T. Schreiber, J. Limpert, and A. Tünnermann, "Femtosecond fiber CPA system emitting 830 W average output power," *Opt. Lett.*, vol. 35, no. 2, pp. 94–96, 2010.

[25] J. Boullet, Y. Zaouter, J. Limpert, S. Petit, Y. Mairesse, B. Fabre, J. Higuet, E. Mével, E. Constant, and E. Cormier, "High-order harmonic generation at a megahertz-level repetition rate directly driven by an ytterbium-doped-fiber chirped-pulse amplification system," *Opt. Lett.*, vol. 34, no. 9, pp. 1489–1491, 2009.

[26] T. V. Andersen, O. Schmidt, C. Bruchmann, J. Limpert, C. Aguergaray, E. Cormier, and A. Tünnermann, "High repetition rate tunable femtosecond pulses and broadband amplification from fiber laser pumped parametric amplifier," *Opt. Exp.*, vol. 14, no. 11, pp. 4765–4773, 2006.

[27] J. Rothhardt, S. Hädrich, D. N Schimpf, J. Limpert, and A. Tünnermann, "High repetition rate fiber amplifier pumped sub-20 fs optical parametric amplifier," *Opt. Exp.*, vol. 15, no. 25, pp. 16729–16736, 2007.

[28] F. Tavella, A. Willner, J. Rothhardt, S. Hädrich, E. Seise, S. Düsterer, T. Tschentscher, H. Schlarb, J. Feldhaus, J. Limpert, A. Tünnermann, and J. Rossbach, "Fiber-amplifier pumped high average power few-cycle pulse non-collinear OPCPA," *Opt. Exp.*, vol. 18, no. 5, pp. 4687–4688, 2010.

[29] M. Hentschel, R. Kienberger, Ch. Spielmann, G. A. Reider, N. Milosevic, T. Brabec, P. Corkum, U. Heinzmann, M. Drescher, and F. Krausz, "Attosecond metrology," *Nature*, vol. 414, no. 6863, pp. 509–513, 2001.

[30] A. Baltuška, Th. Udem, M. Uiberacker, M. Hentschel, E. Goulielmakis, Ch. Gohle, R. Holzwarth, V. S. Yakovlev, A. Scrinzi, T. W Hänsch, and F. Krausz, "Attosecond control of electronic processes by intense light fields," *Nature*, vol. 421, no. 6923, pp. 611–615, 2003.

[31] N. Forget, L. Canova, X. Chen, A. Jullien, and R. Lopez-Martens, "Closed-loop carrier-envelope phase stabilization with an acousto-optic programmable dispersive filter," *Opt. Lett.*, vol. 34, no. 23, pp. 3647–3649, 2009.

[32] T. Wittmann, B. Horvath, W. Helml, M. G Schätzel, X. Gu, A. L. Cavalieri, G. G. Paulus, and R. Kienberger, "Single-shot carrier-envelope phase measurement of few-cycle laser pulses," *Nature Phys.*, vol. 5, no. 5, pp. 357–362, 2009.

[33] S. Koke, C. Grebing, B. Manschwetus, and G. Steinmeyer, "Fast f-to-2f interferometer for a direct measurement of the carrier-envelope phase drift of ultrashort amplified laser pulses," *Opt. Lett.*, vol. 33, no. 21, pp. 2545–2547, 2008.

[34] X. Feng, S. Gilbertson, H. Mashiko, H. Wang, S. D. Khan, M. Chini, Y. Wu, K. Zhao, and Z. Chang, "Generation of isolated attosecond pulses with 20 to 28 femtosecond lasers," *Phys. Rev. Lett.*, vol. 103, no. 18, p. 183901, 2009.

[35] S. Gilbertson, S. D. Khan, Y. Wu, M. Chini, and Z. Chang, "Isolated attosecond pulse generation without the need to stabilize the carrier-envelope phase of driving lasers," *Phys. Rev. Lett.*, vol. 105, no. 9, p. 093902, 2010.

[36] K. S. Budil, P. Salières, M. D. Perry, and A. LHuillier, "Influence of ellipticity on harmonic generation," *Phys. Rev. A*, vol. 48, no. 5, pp. R3437–R3440, 1993.

[37] V. Strelkov, A. Zäir, O. Tcherbakoff, R. López-Martens, E. Cormier, E. Mével, and E. Constant, "Single attosecond pulse production with an ellipticity-modulated driving IR pulse," *J. Phys. B: At. Mol. Opt. Phys.*, vol. 38, no. 10, p. L161, 2005.

[38] Z.-H. Loh, M. Khalil, R. E. Correa, R. Santra, C. Buth, and S. R. Leone, "Quantum state-resolved probing of strong-field-ionized xenon atoms using femtosecond high-order harmonic transient absorption spectroscopy," *Phys. Rev. Lett.*, vol. 98, no. 14, p. 143601, 2007.

[39] Z.-H. Loh and S. R. Leone, "Ultrafast strong-field dissociative ionization dynamics of CH_2Br_2 probed by femtosecond soft x-ray transient absorption spectroscopy," *J. Chem. Phys.*, vol. 128, no. 20, p. 204302, 2008.

[40] T. Pfeifer, M. J. Abel, P. M. Nagel, A. Jullien, Z.-H. Loh, M. J. Bell, D. M. Neumark, and S. R. Leone, "Time-resolved spectroscopy of attosecond quantum dynamics," *Chem. Phys. Lett.*, vol. 463, no. 1–3, pp. 11–24, 2008.

[41] T. Remetter, P. Johnsson, J. Mauritsson, K. Varjú, Y. Ni, F. Lépine, E. Gustafsson, M. Kling, J. Khan, R. López-Martens, K. J. Schafer, M. J. J. Vrakking, and A. L'Huillier, "Attosecond electron wave packet interferometry," *Nat. Phys.*, vol. 2, no. 5, pp. 323–326, 2006.

[42] G. Sansone, E. Benedetti, J. P. Caumes, S. Stagira, C. Vozzi, M. Nisoli, L. Poletto, P. Villoresi, V. Strelkov, I. Sola, L. B. Elouga, A. Zaïr, E. Mével, and E. Constant, "Shaping of attosecond pulses by phase-stabilized polarization gating," *Phys. Rev. A*, vol. 80, no. 6, p. 063837, 2009.

[43] H. Hasegawa, E. J. Takahashi, Y. Nabekawa, K. L. Ishikawa, and K. Midorikawa, "Multiphoton ionization of He by using intense high-order harmonics in the soft-X-ray region," *Phys. Rev. A*, vol. 71, no. 2, p. 023407, 2005.

[44] N. Miyamoto, M. Kamei, D. Yoshitomi, T. Kanai, T. Sekikawa, T. Nakajima, and S. Watanabe, "Observation of two-photon above-threshold

ionization of rare gases by XUV harmonic photons," *Phys. Rev. Lett.*, vol. 93, no. 8, p. 083903, 2004.
[45] Y. Nabekawa, H. Hasegawa, E. J. Takahashi, and K. Midorikawa, "Production of doubly charged helium ions by two-photon absorption of an intense sub-10-fs soft X-ray pulse at 42 eV photon energy," *Phys. Rev. Lett.*, vol. 94, no. 4, p. 043001, 2005.
[46] P. Tzallas, D. Charalambidis, N. A. Papadogiannis, K. Witte, and G. D. Tsakiris, "Direct observation of attosecond light bunching," *Nature*, vol. 426, no. 6964, pp. 267–271, 2003.
[47] V. S. Yakovlev, J. Gagnon, N. Karpowicz, and F. Krausz, "Attosecond streaking enables the measurement of quantum phase," *Phys. Rev. Lett.*, vol. 105, no. 7, p. 073001, 2010.
[48] Y. Mairesse and F. Quéré, "Frequency-resolved optical gating for complete reconstruction of attosecond bursts," *Phys. Rev. A*, vol. 71, no. 1, p. 011401, 2005.
[49] M. Kitzler, N. Milosevic, A. Scrinzi, F. Krausz, and T. Brabec, "Quantum theory of attosecond XUV pulse measurement by laser dressed photoionization," *Phys. Rev. Lett.*, vol. 88, no. 17, p. 173904, 2002.
[50] J. Itatani, F. Quéré, G. L. Yudin, M. Yu. Ivanov, F. Krausz, and P. B. Corkum, "Attosecond streak camera," *Phys. Rev. Lett.*, vol. 88, no. 17, p. 173903, 2002.
[51] R. Kienberger, E. Goulielmakis, M. Uiberacker, A. Baltuŝka, V. Yakovlev, F. Bammer, A. Scrinzi, Th. Westerwalbesloh, U. Kleineberg, U. Heinzmann, M. Drescher, and F. Krausz, "Atomic transient recorder," *Nature*, vol. 427, no. 6977, pp. 817–821, 2004.
[52] R. Trebino, K. W De Long, D. N. Fittinghoff, J. N. Sweetser, M. A Krumbügel, B. A. Richman, and D. J. Kane, "Measuring ultrashort laser pulses in the time-frequency domain using frequency-resolved optical gating," *Rev. Sci. Instrum.*, vol. 68, no. 9, p. 3277, 1997.
[53] G. Sansone, E. Benedetti, F. Calegari, C. Vozzi, L. Avaldi, R. Flammini, L. Poletto, P. Villoresi, C. Altucci, R. Velotta, S. Stagira, S. De Silvestri, and M. Nisoli, "Isolated single-cycle attosecond pulses," *Science*, vol. 314, no. 5798, pp. 443–446, 2006.
[54] F. Quéré, J. Itatani, G. L. Yudin, and P. B. Corkum, "Attosecond spectral shearing interferometry," *Phys. Rev. Lett.*, vol. 90, no. 7, p. 073902, 2003.
[55] C. Iaconis and I. A. Walmsley, "Spectral phase interferometry for direct electric-field reconstruction of ultrashort optical pulses," *Opt. Lett.*, vol. 23, no. 10, pp. 792–794, 1998.
[56] E. Cormier, I. A. Walmsley, E. M. Kosik, A. S. Wyatt, L. Corner, and L. F. DiMauro, "Self-referencing, spectrally, or spatially encoded spectral interferometry for the complete characterization of attosecond electromagnetic pulses," *Phys. Rev. Lett.*, vol. 94, no. 3, p. 033905, 2005.
[57] Y. Mairesse, O. Gobert, P. Breger, H. Merdji, P. Meynadier, P. Monchicourt, M. Perdrix, P. Salières, and B. Carré, "High harmonic XUV spectral phase interferometry for direct electric-field reconstruction," *Phys. Rev. Lett.*, vol. 94, no. 17, p. 173903, 2005.
[58] N. Dudovich, O. Smirnova, J. Levesque, Y. Mairesse, M. Yu. Ivanov, D. M. Villeneuve, and P. B. Corkum, "Measuring and controlling the birth of attosecond XUV pulses," *Nat. Physics*, vol. 2, no. 11, pp. 781–786, 2006.
[59] M. Chini, S. Gilbertson, S. D. Khan, and Z. Chang, "Characterizing ultrabroadband attosecond lasers," *Opt. Exp.*, vol. 18, no. 12, pp. 13006–13016, 2010.
[60] P. M. Paul, E. S. Toma, P. Breger, G. Mullot, F. Augé, Ph. Balcou, H. G. Muller, and P. Agostini, "Observation of a train of attosecond pulses from high harmonic generation," *Science*, vol. 292, no. 5522, pp. 1689–1692, 2001.
[61] V. Véniard, R. Taïeb, and A. Maquet, "Two-color multiphoton ionization of atoms using high-order harmonic radiation," *Phys. Rev. Lett.*, vol. 74, no. 21, pp. 4161–4164, 1995.
[62] V. Véniard, R. Taïeb, and A. Maquet, "Phase dependence of (N + 1)-color (N > 1) IR-UV photoionization of atoms with higher harmonics," *Phys. Rev. A*, vol. 54, no. 1, pp. 721–728, 1996.
[63] J. Mauritsson, T. Remetter, M. Swoboda, K. Klünder, A. LHuillier, K. J. Schafer, O. Ghafur, F. Kelkensberg, W. Siu, P. Johnsson, M. J. J. Vrakking, I. Znakovskaya, T. Uphues, S. Zherebtsov, M. F. Kling, F. Lépine, E. Benedetti, F. Ferrari, G. Sansone, and M. Nisoli, "Attosecond electron spectroscopy using a novel interferometric pump-probe technique," *Phys. Rev. Lett*, vol. 105, no. 5, p. 053001, 2010.
[64] A. T. J. B. Eppink and D. H. Parker, "Velocity map imaging of ions and electrons using electrostatic lenses: Application in photoelectron and photofragment ion imaging of molecular oxygen," *Rev. Sci. Instrum.*, vol. 68, no. 9, p. 3477, 1997.
[65] M. J. J.Vrakking, "An iterative procedure for the inversion of two-dimensional ion/photoelectron imaging experiments," *Rev. Sci. Instrum.*, vol. 72, no. 11, p. 4084, 2001.
[66] M. F. Kling, Ch. Siedschlag, A. J. Verhoef, J. I. Khan, M. Schultze, Th. Uphues, Y. Ni, M. Uiberacker, M. Drescher, F. Krausz, and M. J. J. Vrakking, "Control of electron localization in molecular dissociation," *Science*, vol. 312, no. 5771, pp. 246–248, 2006.
[67] E. Péronne, M. D. Poulsen, Ch. Z. Bisgaard, H. Stapelfeldt, and Tamar Seideman, "Nonadiabatic alignment of asymmetric top molecules: Field-free alignment of iodobenzene," *Phys. Rev. Lett.*, vol. 91, no. 4, p. 043003, 2003.
[68] S. De, I. Znakovskaya, D. Ray, F. Anis, N. G. Johnson, I. A. Bocharova, M. Magrakvelidze, B. D. Esry, C. L. Cocke, I. V. Litvinyuk, and M. F. Kling, "Field-free orientation of CO molecules by femtosecond two-color laser fields," *Phys. Rev. Lett.*, vol. 103, no. 15, p. 153002, 2009.
[69] O. J. Ghafur, W. JSiu, P. JJohnsson, M. F. Kling, M. JDrescher, and M. JJ. J. Vrakking, "A velocity map imaging detector with an integrated gas injection system," *Rev. Sci. Instrum.*, vol. 80, no. 3, p. 033110, 2009.
[70] G. Gademann, Y. Huismans, A. Gijsbertsen, J. Jungmann, J. Visschers, and M. J J.Vrakking, "Velocity map imaging using an in-vacuum pixel detector," *Rev. Sci. Instrum.*, vol. 80, no. 10, p. 103105, 2009.
[71] H. Stapelfeldt and T. Seideman, "Aligning molecules with strong laser pulses," *Rev. Mod. Phys.*, vol. 75, no. 2, pp. 543–557, 2003.
[72] L. S. Cederbaum, J. Zobeley, and F. Tarantelli, "Giant intermolecular decay and fragmentation of clusters," *Phys. Rev. Lett.*, vol. 79, no. 24, pp. 4778–4781, 1997.
[73] T. Jahnke, H. Sann, T. Havermeier, K. Kreidi, C. Stuck, M. Meckel, M. Schöffler, N. Neumann, R. Wallauer, S. Voss, A. Czasch, O. Jagutzki, A. Malakzadeh, F. Afaneh, Th. Weber, H. Schmidt-Böcking, and R. Dörner, "Ultrafast energy transfer between water molecules," *Nat. Physics*, vol. 6, no. 2, pp. 139–142, 2010.
[74] M. Mucke, M. Braune, S. Barth, M. Förstel, T. Lischke, V. Ulrich, T. Arion, U. Becker, A. Bradshaw, and U. Hergenhahn, "A hitherto unrecognized source of low-energy electrons in water," *Nat. Phys.*, vol. 6, no. 2, pp. 143–146, 2010.
[75] T. Jahnke, A. Czasch, M. S Schöffler, S. Schössler, A. Knapp, M. Käsz, J. Titze, C. Wimmer, K. Kreidi, R. E. Grisenti, A. Staudte, O. Jagutzki, U. Hergenhahn, H. Schmidt-Böcking, and R. Dörner, "Experimental observation of interatomic coulombic decay in neon dimers," *Phys. Rev. Lett.*, vol. 93, no. 16, p. 163401, 2004.
[76] A. S. Sandhu, E. Gagnon, R. Santra, V. Sharma, W. Li, P. Ho, P. Ranitovic, C. L. Cocke, M. M. Murnane, and H. C. Kapteyn, "Observing the creation of electronic feshbach resonances in soft X-ray-induced O_2 dissociation," *Science*, vol. 322, no. 5904, pp. 1081–1085, 2008.
[77] E. Gagnon, P. Ranitovic, X.-M. Tong, C. L. Cocke, M. M. Murnane, H. C. Kapteyn, and A. S. Sandhu, "Soft X-ray-driven femtosecond molecular dynamics," *Science*, vol. 317, no. 5843, pp. 1374–1378, 2007.
[78] F. Remacle and R. D. Levine, "An electronic time scale in chemistry," *PNAS*, vol. 103, no. 18, pp. 6793–6798, 2006.
[79] J. Breibach and L. S. Cederbaum, "Migration of holes: Formalism, mechanisms, and illustrative applications," *J. Chem. Phys.*, vol. 118, no. 9, p. 3983, 2003.
[80] A. I. Kuleff and L. S. Cederbaum, "Charge migration in different conformers of glycine: The role of nuclear geometry," *Chem. Phys.*, vol. 338, no. 2–3, pp. 320–328, 2007.
[81] F. Filsinger, U. Erlekam, G. von Helden, J. Küpper, and G. Meijer, "Selector for structural isomers of neutral molecules," *Phys. Rev. Lett.*, vol. 100, no. 13, p. 133003, 2008.
[82] K. L. Ishikawa and K. Midorikawa, "Above-threshold double ionization of helium with attosecond intense soft X-ray pulses," *Phys. Rev. A*, vol. 72, no. 1, p. 013407, 2005.
[83] J. Feist, S. Nagele, R. Pazourek, E. Persson, B. I. Schneider, L. A. Collins, and J. Burgdörfer, "Probing electron correlation via attosecond XUV pulses in the two-photon double ionization of helium," *Phys. Rev. Lett.*, vol. 103, no. 6, p. 063002, 2009.
[84] U. Fano, "Effects of configuration interaction on intensities and phase shifts," *Phys. Rev.*, vol. 124, no. 6, pp. 1866–1878, 1961.
[85] M. Wickenhauser, J. Burgdörfer, F. Krausz, and M. Drescher, "Time resolved fano resonances," *Phys. Rev. Lett.*, vol. 94, no. 2, p. 023002, 2005.
[86] L. Argenti and E. Lindroth, "Ionization branching ratio control with a resonance attosecond clock," *Phys. Rev. Lett.*, vol. 105, no. 5, p. 053002, 2010.
[87] P. Johnsson, J. Mauritsson, T. Remetter, A. L. Huillier, and K. J. Schafer, "Attosecond control of ionization by wave-packet interference," *Phys. Rev. Lett.*, vol. 99, no. 23, p. 233001, 2007.

[88] J. L. Krause, K. J. Schafer, and K. C. Kulander, "High-order harmonic generation from atoms and ions in the high intensity regime," *Phys. Rev. Lett.*, vol. 68, no. 24, pp. 3535–3538, 1992.
[89] P. Riviére, O. Uhden, U. Saalmann, and J. M. Rost, "Strong field dynamics with ultrashort electron wave packet replicas," *New J. Phys.*, vol. 11, p. 053011, 2009.
[90] P. Ranitovic, X. M Tong, B. Gramkow, S. De, B. DePaola, K. P Singh, W. Cao, M. Magrakvelidze, D. Ray, I. Bocharova, H. Mashiko, A. Sandhu, E. Gagnon, M. M Murnane, H. C. Kapteyn, I. Litvinyuk, and C. L Cocke, "IR-assisted ionization of helium by attosecond extreme ultraviolet radiation," *New J. Phys.*, vol. 12, p. 013008, 2010.
[91] M. Swoboda, T. Fordell, K. Klünder, J. M. Dahlström, M. Miranda, C. Buth, K. J. Schafer, J. Mauritsson, A. LHuillier, and M. Gisselbrecht, "Phase measurement of resonant two-photon ionization in helium," *Phys. Rev. Lett.*, vol. 104, no. 10, p. 103003, 2010.
[92] I. J. Sola, E. Mével, L. Elouga, E. Constant, V. Strelkov, L. Poletto, P. Villoresi, E. Benedetti, J. P. Caumes, S. Stagira, C. Vozzi, G. Sansone, and M. Nisoli, "Controlling attosecond electron dynamics by phasestabilized polarization gating," *Nature Phys.*, vol. 2, no. 5, pp. 319–322, 2006.
[93] G. Sansone, E. Benedetti, C. Vozzi, S. Stagira, and M. Nisoli, "Attosecond metrology in the few-optical-cycle regime," *New J. Phys.*, vol. 10, p. 025006, 2008.
[94] N. N. Choi, T. F. Jiang, T. Morishita, M.-H. Lee, and C. D. Lin, "Theory of probing attosecond electron wave packets via two-path interference of angleresolved photoelectrons," *Phys. Rev. A*, vol. 82, no. 1, p. 013409, 2010.

Giuseppe Sansone received the Ph.D. degree in physics (with an experimental thesis on the effects of the Carrier-Envelope Phase CEP on the HHG process) from the Politecnico of Milan, Piazza L. da Vinci, Milan, Italy, in 2004.

In 2007, he was with the Laser Technology Laboratory at RIKEN, Wako Saitama, Japan, as a short term Postdoctoral Research Fellow of the Japan Society for the Promotion of Science foundation. In 2008, he was with the Department of Chemistry, Tokyo University, as a Visiting Scientist. From 2009 to 2010, he was with the Max Planck Institut für Kernphysik, Heidelberg, as an Alexander von Humboldt Fellow. He is currently an Assistant Professor of the Faculty of the Politecnico of Milano. His research interests include the characterization of attosecond electron dynamics by coincidence measurements of charged particles.

Francesca Calegari was born in Italy, on January 11, 1981. She received the Master's degree (*cum laude*) in physics from the Universitá degli Studi di Milano, Milan, Italy, in 2005, and the Ph.D. degree in physics from Politecnico di Milano, Milan, Italy, in 2009.

She is currently a Postdoctoral Researcher at the Physics Department, Politecnico di Milano. She is a coauthor of about 30 research papers published in international journals. Her current research interests include attosecond physics, coherent XUV generation from atom and molecules, and ultrafast laser technology.

Mauro Nisoli received the degree (*cum laude*) in electronic engineering from the Politecnico di Milano, Milan, Italy, in 1990.

From 1991 to 2001, he was a Researcher of the National Research Council (CNR) with the Center of Quantum Electronic and Electronic Instrumentation. Since 2001, he has been as Associate Professor (Physics of Matter) of the Faculty of Politecnico di Milano . He is a coauthor of about 140 research papers published in international journals, one patent, and several invited and tutorial communications at international meetings and schools. His current research interests include ultrashort-pulse laser technology; attosecond physics: generation, characterization and application of isolated attosecond pulses; control and real-time observation of electronic motion in atoms and molecules.